

Nonspecific Protein Adsorption at the Single Molecule Level Studied by Atomic Force Microscopy

Peter Schön,^{*,†} Martin Görlich,[†] Michiel J. J. Coenen,[†] Hans A. Heus,[‡] and Sylvia Speller[†]

Radboud University Nijmegen, Institute for Molecules and Materials, Toernooiveld 1, 6525 ED Nijmegen, the Netherlands

Received January 29, 2007. In Final Form: July 9, 2007

Liquid tapping atomic force microscopy was used to study the nonspecific adsorption of horse spleen ferritin at a bare gold surface at single molecule resolution. The majority of ferritin molecules adsorbed irreversibly on gold surfaces in accordance with the random sequential adsorption (RSA) mechanism frequently used to describe irreversible adsorption processes. However, the time-resolved data also reveal events that go beyond the RSA model, i.e., lateral mobility and fragility of some molecules, resulting in desorption, chain formation, and subunit dissociation. Scanning effects of the AFM tip were observed, resulting in diminished protein coverage in the scanned area.

The nonspecific adsorption of proteins at solid surfaces plays a central role in many technical applications including biosensors, medical implants, nonfouling surfaces in food industry, and marine environments. Despite the technological importance and large number of fundamental studies, protein adsorption is still not well understood at the molecular level.^{1,2} Besides Langmuir-type and multilayer adsorption, so-called random sequential adsorption (RSA) is very often observed, indicating the irreversibility of the process: molecules once adsorbed do not show any lateral mobility or desorption and the occupied area remains completely excluded for other molecules.^{3,4}

Despite the extremely high sensitivity of some of the techniques used to investigate protein adsorption, enabling the detection of submonolayer adsorption of proteins, they all lack spatial resolution of the adsorption process.⁵ Recently atomic force microscopy has been used to study protein adsorptions at different solid surfaces in situ, which provided spatial resolution of the fractional growth of protein layers and aggregation of adsorbed proteins.^{6–8} To the best of our knowledge there is no in situ study of protein adsorption in real space and time with single molecule resolution so far. In this work we use atomic force microscopy to study the nonspecific adsorption of horse spleen ferritin at a gold surface from solution on the nanoscale in real space and time.

Ferritins are a class of iron storage proteins found in bacterial, plant, and animal cells. Ferritins form hollow shells with 80 Å diameter cavities in which 2000 to 4500 Fe(III) ions can be stored as an inorganic complex.⁹ All ferritins are composed of 24 protein subunits, and depending on the organism, ferritin molecules measure up to 12 nm in total diameter, with several channels that appear to mediate selectively iron transport to and from the interior. The inner diameter of the protein shell is ca.

8 nm. The nonspecific adsorption of ferritin at various model surfaces has been studied in detail, both experimentally and theoretically.^{10–14} Ferritin layers on gold and modified gold surfaces have been investigated by AFM in air.^{15,16} High-resolution AFM topographies of ferritin molecules have been obtained on modified silicon and mica.^{17,18} In our AFM study, ferritin molecules were deposited from solutions using volumes of 60 μL . The total gold area measured ca. 0.3–0.4 cm^2 , and the additional surface from the supporting glass substrate and the liquid cell were roughly 1 cm^2 . Continuous scanning over a subsection of $3 \times 3 \mu\text{m}^2$ at 1.6 Hz scan rate was used to acquire a series of consecutive AFM images, every 320 s, in liquid tapping mode. After obtaining stable imaging conditions in the absence of ferritin, a small volume of protein stock solution was administered to the buffer droplet using a Hamilton microliter syringe. During continuous scanning, the solution was carefully mixed by repetitive push/pull of the measurement solution. Introducing the syringe into the measurement cell caused a disturbance of the topography signal (the distinct horizontal lines in Figure 1), which recovered quickly after withdrawing the syringe. Protein addition, mixing, and stabilization of the topography signal roughly took 1 min. After ca. 1 min, the first protrusion was detected in the upper right of the topographic image (Figure 1.1), which we interpret as a single adsorbed protein molecule.

The number of protrusions continuously increased with scanning time (Figure 1.2.–1.3 and Supporting Information movie). In total 11 topographic images were collected at a protein concentration of 0.36 $\mu\text{g}/\text{mL}$ until no significant increase in adsorption could be observed. The majority of the observed individual signatures, due to individual proteins, exhibit a fwhm of 20–40 nm and an apparent height of 10 ± 2 nm. The apparent width is considerably larger than the true dimension, mainly due to AFM tip broadening. Apart from these signatures, we find smaller ones measuring only 3 ± 1 nm in height. These could

* To whom correspondence should be addressed. E-mail: p.schoen@science.ru.nl.

[†] Scanning Probe Microscopy Laboratories.

[‡] Biophysical Chemistry.

- (1) Ramsden, J. J. *Chem. Soc. Rev.* **1995**, *24*, 73.
- (2) Andrade, V. H.; Wei, A. P. *Pure Appl. Chem.* **1992**, *64*, 1777.
- (3) Schaaf, P.; Voegel, J. C.; Senger, B. *J. Phys. Chem. B* **2000**, *104*, 2204.
- (4) Seigel, R. R.; Harder, P.; Dahint, R.; Grunze, M.; Josse, F.; Mrksich, M.; Whitesides, G. M. *Anal. Chem.* **1997**, *69*, 3321.
- (5) Ramsden, J. J. *Q. Rev. Biophys.* **1994**, *27*, 41.
- (6) Kim, D. T.; Blanch, H. W.; Radke, C. J. *Langmuir* **2002**, *18*, 5841.
- (7) McMaster, T. J.; Miles, M. J.; Shewry, P. R.; Tatham, A. S. *Langmuir* **2000**, *16*, 1463.
- (8) Rieu, J. P.; Ronzon, F.; Roux, B. *Thin Solid Films* **2002**, *406*, 241.
- (9) Aisen, P.; Listowsky, I. *Annu. Rev. Biochem.* **1980**, *49*, 357.

- (10) Feder, J.; Giaever, I. *J. Colloid Interface Sci.* **1980**, *78*, 144.
- (11) Nygren, H. *Biophys. J.* **1993**, *65*, 1508.
- (12) Nygren, H.; Arwin, H.; Welinklintstrom, S. *Colloids Surf. A* **1993**, *76*, 87.
- (13) Nygren, H.; Stenberg, M. *Biophys. Chem.* **1990**, *38*, 67.
- (14) Nygren, H.; Stenberg, M. *Biophys. Chem.* **1990**, *38*, 77.
- (15) Caruso, F.; Furlong, D. N.; Kingshott, P. *J. Colloid Interface Sci.* **1997**, *186*, 129.
- (16) Tominaga, M.; Ohira, A.; Yamaguchi, Y.; Kunitake, M. *J. Electroanal. Chem.* **2004**, *566*, 323.
- (17) Ohnishi, S.; Hara, M.; Furuno, T.; Sasabe, H. *Biophys. J.* **1992**, *63*, 1425.
- (18) Yang, J.; Mou, J. X.; Shao, Z. F. *Biochim. Biophys. Acta* **1994**, *1199*, 105.

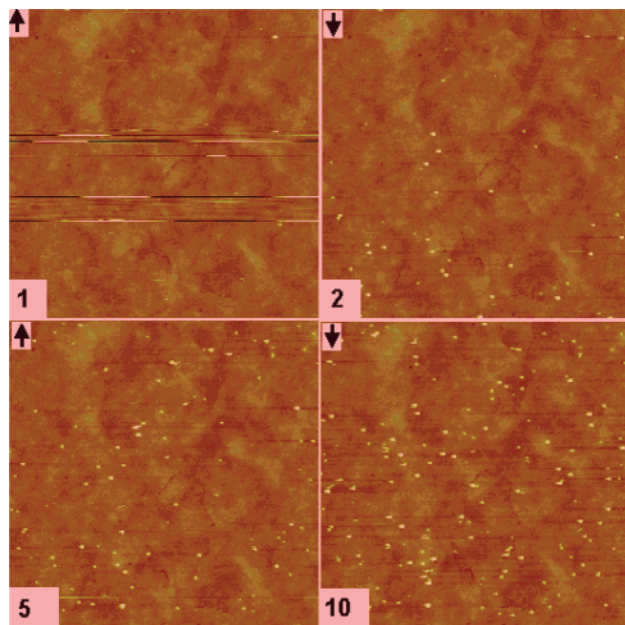


Figure 1. Topographic images no 1,2,5,10 of a consecutive series of 11 images obtained upon addition of ferritin solution (final concentration $0.36 \mu\text{g/mL}$), scan rate: 1.606 Hz , frame size: $3 \mu\text{m} \times 3 \mu\text{m}$, $z = 20 \text{ nm}$. Arrows indicate scanning directions.

originate from the varying iron mineral content of the ferritin, rendering the molecules partly hollow and therefore more compressible by AFM tip interaction. Also denaturation of the protein can induce subunit dissociation yielding smaller objects. Similar heights have been reported for dried ferritin layers in air.¹⁵

Ferritin molecules contain 2 cysteins per subunit, enabling strong binding to gold surfaces through covalent thiol–gold linkages, and most of the observed particles remain stuck at their initial positions. Apparently, binding forces of the protein–surface exceed possible protein–AFM tip interactions in liquid tapping mode. However, apart from adsorption, some other striking events are observed, like desorption, dissociation, and lateral movement of individual ferritin molecules (Figure 2, panels A and B and Supporting Information movie).

At a 10-fold higher protein concentration ($3.6 \mu\text{g/mL}$), the first protrusions appear ca. 1 to 10 s after protein administration, of which the amount increases at a significantly higher rate compared to the low protein concentration. After ca. 30 min, the adsorption saturates with a coverage of roughly 5%. At this higher protein concentration, chains of 4–8 protrusions are formed, covering distances of ca. 100–200 nm (Figure 2C). We speculate that most probably the gold topography (step edge) is the reason for this chain formation and not intermolecular interactions, because the distances between the individual molecules of $40 \pm 5 \text{ nm}$ are too large.

In the following, we evaluate the adsorption kinetics and the radial distribution function. We used ImageJ (1.37v) to count the number of particles and extract the x – y positions of particle centers in each image. Even with our highest observed coverage, we find no appreciable maximum in the radial distribution or pair correlation function (see Figure 4 in the Supporting Information). Johnson et al. used higher ferritin concentration and differently charged surfaces, and maxima in the radial distribution functions were observed.¹⁹ Significant pair correlation has also been observed at very low coverage, e.g., with strongly

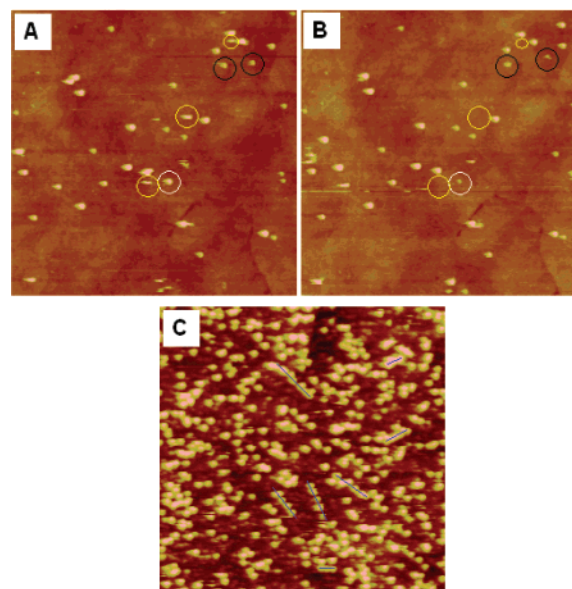


Figure 2. (A) Topographic image no 9 of the experiment shown in Figure 1 with indications of different rare events observed in comparison with the consecutive image no. 10 (B) marked with circles. White: dissociation, black: lateral movement, green: desorption. (C) Topographic image no. 7 of a series, conducted at $3.6 \mu\text{g/mL}$, with ferritin chains indicated. All images $1.5 \mu\text{m} \times 1.5 \mu\text{m}$, $z = 20 \text{ nm}$.

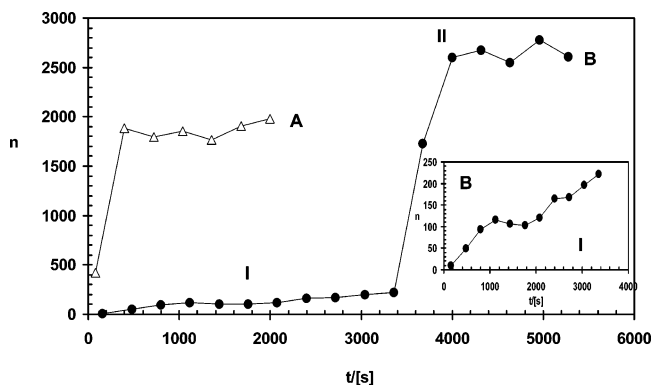


Figure 3. protein adsorption kinetics as deduced from the total number of counted particles on $3 \times 3 \mu\text{m}^2$ as function of time and of ferritin solution concentration; A (open triangles): ferritin concentration: $3.6 \mu\text{g/mL}$; B (black circles): two step adsorption experiment; (I) ferritin concentration: $0.36 \mu\text{g/mL}$; (II) $3.6 \mu\text{g/mL}$; inset: zoom in of the initial adsorption kinetics (B, I) at a ferritin concentration of $0.36 \mu\text{g/mL}$.

charged particles from Adamczyk; thus, we can conclude that there is no attractive interaction between the ferritin particles in our experiments.²⁰ The protein adsorption kinetics are depicted in Figure 3. Here we evaluated image-wise; therefore, the time resolution is low (320 s) but sufficient. The adsorption kinetics show a root(time) behavior in the initial phase indicating diffusion control at the beginning of the experiment (data not shown). An interesting observation is that at low protein solution concentration the coverage usually drops again after having achieved a maximum coverage after a couple of frames (ca. 1000 s, see Figure 3, inset). Obviously substantial desorption occurs in this initial stage. This could be induced by the force due to the vicinity of the AFM probe or by unfavorable adsorption geometry in that the ferritin is bound only weakly. Increasing the protein concentration leads to significantly enhanced adsorption rates.

(19) Johnson, C. A.; Yuan, Y.; Lenhoff, A. M. *J. Colloid Interface Sci.* **2000**, *223*, 261.

(20) Adamczyk, Z.; Jaszczolt, K.; Siwek, B.; Weroni, P. *J. Chem. Phys.* **2004**, *120*, 11155.

Saturation is then reached after ca. 10 min, although still a moderate increase of coverage can be detected at greater time values. At the higher protein solution concentration (Figure 3, A + B II), significantly higher adsorption rates can be observed accompanied by saturation after roughly 10 min. The initial adsorption rate at the low ferritin concentration (Figure 3, B I) equals roughly 1 ferritin molecule every 10 s, whereas the experiments at the higher concentration (Figure 3, A + B II) show rates of roughly 5 ferritin molecules adsorbed per second on average on the observed area of $9 \mu\text{m}^2$.

The low saturation coverage of the surface is probably influenced by AFM tip shadowing. Scanning a larger area after the initial adsorption experiment shows a ca. 2-fold higher protein density compared to the area where scanning was initially performed (Supporting Information, Figure 2). This is attributed to lateral removal of adsorbed molecules or AFM tip interference during scanning. The AFM tip shields the gold surface and the amplitude of the cantilever is in the regime of the ferritin diameter so that most of the time the tip is too close to the surface and molecules cannot slip/glide in-between. Stirring effects from cantilever and tip can also contribute to reduce the adsorption probability. We mention that tapping mode imaging reduces lateral shear forces here in comparison to contact mode imaging and thus minimizes mechanical manipulation of adsorbed proteins. However, occasional adsorption of proteins at the AFM tip is quite probable: sometimes a significant enhancement of the spherical signature during a number of scans was observed (Supporting Information, Figure 3). Protein adsorption to the AFM tip increases its effective radius and enlarges the apparent width (fwhm) of individual particles while their heights remain unaffected.

In conclusion, the experiments described herein demonstrate as a proof-of-principle that physisorption of proteins at surfaces can be studied at the single molecule level by liquid tapping AFM and provide insight into the mechanism of binding. The majority of ferritin molecules adsorbed irreversible on gold surfaces in accordance with the random sequential adsorption (RSA) mechanism frequently used to describe irreversible adsorption processes. However, the time-resolved data also reveal events that go beyond the RSA model, i.e., lateral mobility and fragility of some molecules, resulting in desorption, chain formation, and subunit dissociation. Scanning effects of the AFM tip were observed, resulting in diminished protein coverage in the scanned area. Further optimization and adaptation of the AFM setup and experiments should provide detailed mechanistic insight into protein adsorption under physiological conditions that cannot be obtained by other techniques.

Acknowledgment. This work was supported by FOM/ALW and by NanoNed, the Dutch nanotechnology program of the Ministry of Economic Affairs. Helpful discussions with A. Fasolino (Radboud University Nijmegen) are gratefully acknowledged.

Supporting Information Available: Sample preparation, buffer, and AFM conditions. Five figures and four movies, showing the entire adsorption experiments, the lateral mobility events of single objects, and the effect of AFM tip scanning and shadowing, adsorption kinetics, and radial distribution functions. This information is available free of charge via the Internet at <http://pubs.acs.org>.

LA700236Z